Extrapolation of Time-Domain Responses from Three-Dimensional Conducting Objects Utilizing the Matrix Pencil Technique

Raviraj S. Adve, *Student Member, IEEE*, Tapan Kumar Sarkar, *Fellow, IEEE*, Odilon Maroja C. Pereira-Filho, *Student Member, IEEE*, and Sadasiva M. Rao, *Senior Member, IEEE*

***Abstract*— In this paper, we use the matrix pencil approach to extrapolate time-domain responses from three-dimensional (3-D) conducting objects that arise in the numerical solution of electromagnetic field problems. By modeling the time functions as a sum of complex exponentials, we can eliminate some of the instabilities that arise in late times for the electric-field integral equation in the time domain. However, this method can also be utilized for extending the responses obtained using a finite-difference time-domain (FDTD) formulation.**

***Index Terms*— Time-domain analyses.**

I. Introduction

In most of computational electromagnetics the solution technique assumes a time-harmonic behavior for all field quantities. This implies that the solution is in the frequency domain. The principal reason for this has been that the frequency domain approach is more tractable analytically. Time-domain solutions are then found using an inverse Fourier transform.

However, with the increasing speed and memory of digital computers, many scattering problems are being performed in the time domain. There are three basic reasons for time-domain modeling [1]. In certain electromagnetic problems, fewer arithmetic operations are required when the solution approach is in the time domain. Second, in seeking broad-band information, a time-domain model is intrinsically a better choice. The transient response obtained is limited only by the bandwidth of the excitation and the spatial discretization. In such a case, a frequency-domain model would require the solution to be performed at each frequency point of interest.

The other reason for time-domain modeling is that problems involving nonlinear media can usually be modeled easily in the time domain. This advantage holds true for time-varying media. Handling nonlinear media and time-varying media can be extremely difficult in the frequency domain. Another benefit of time-domain analysis is that gating can be used to eliminate unwanted reflections.

Manuscript received July 28, 1995; revised November 27, 1995.

R. S. Adve, T. K. Sarkar, and O. M. C. Pereira-Filho are with the Department of Electrical and Computer Engineering, Syracuse University, Syracuse, NY 13244 USA.

S. M. Rao is with the Department of Electrical Engineering, Auburn University, Auburn, AL 36849 USA.

Publisher Item Identifier S 0018-926X(97)01055-7.

Time-domain solutions can be formulated as differential equations or integral equations. In both approaches, the infinite time domain analytical description of the problem is reduced to a finite domain, numerical description. In a differential equation formulation, the unknowns are field values on a grid covering the entire region of interest. For an integral-equation formulation, the unknowns are confined to a surface. In a scattering problem where the space is usually unbounded, the differential equation approach requires that the discretization grid be terminated at a suitable distance from the scatterer in a suitable fashion. For the integral equation approach we will need significantly fewer unknowns.

The time-domain formulation using integral equations usually results in the method of marching on time (MOT). Here, the value of an unknown at any given time t_1 is dependent on the excitation at t_1 and the values of the unknowns for $t < t_1$. By properly choosing a time step, an explicit solution for the unknowns can be obtained. However, MOT algorithms suffer from some serious defects. One main disadvantage is the persistent presence of late-time high-frequency oscillations. These oscillations are present even when the time step is chosen such that the Courant stability condition is satisfied [2]. Many different approaches have been suggested to overcome these instabilities [3]–[5]. For example, the approach proposed in [6] utilizes a relaxation method. In [7], a conjugate gradient approach is applied by converting the hyperbolic partial differential equation to an elliptical one (a boundary value problem), whereas in [8], a filtering technique has been proposed to eliminate late-time instabilities.

In this work, we present the use of the matrix pencil algorithm to eliminate the late-time instabilities. The approach is to model the free response (the time-domain response after the excitation has died down) as a sum of complex exponentials. The input to the matrix pencil algorithm is the output from the MOT code for a short period of time after the excitation has died down. Usually, in this short period the instabilities have not set in. Modeling the free response as a sum of complex exponentials results in a stable time-domain response for all times. Hence, we use the matrix pencil to eliminate the late-time high-frequency oscillations. Also, since now the MOT code needs to be run for a short time after the excitation dies down, this approach results in significant savings in program execution time. It has been assumed in this paper that we are dealing with three-dimensional conducting

bodies. For two-dimensional structures, one has to (in addition) deal with a branch cut [9].

In this paper, we assume that we have been given the currents on the scatterer as a response to a known excitation. These currents have been calculated as a function of time over a limited region. The details of a MOT algorithm can be obtained in any of the numerous references listed in [1] or from [2].

In the next section, we present the matrix pencil as a mathematical tool to model a time-domain sequence as a sum of complex exponentials. We then present the application of the MOT and matrix pencil algorithms to some examples. Finally, some conclusions as to the efficacy of our method are drawn.

II. Matrix Pencil

Consider a function $y(t)$ that represents the current at a particular position on a three-dimensional conduction scatterer as a function of time. This current is the transient response to some known excitation. We model the function, after the excitation had died down, as a sum of complex exponentials.

$$y(t) = \sum_{i=1}^{M} R_i e^{s_i t}. \tag{1}$$

Such a model is valid because the scatterer can be treated as a linear time-invariant (LTI) system. It is well known that for a LTI system, the eigenfunctions of the transfer operator are of the form $e^{s_i t}$ where s_i are the poles of the system. Also, these eigenfunctions are complete in the output space, i.e., any output response can be modeled as a weighted sum of these eigenfunctions.

As a result of the MOT algorithm, N samples of this function are available at intervals of T_s. Therefore, (1) can be written as

$$\begin{aligned} y_k &= y(kT_s + T_0) \\ &= \sum_{i=1}^{M} R_i z_i^k \qquad k = 0, \cdots, N-1 \end{aligned} \tag{2}$$

where T_0 has been introduced to make sure that the response is the free response of the system after the excitation has died down. In addition

$$\begin{aligned} z_i &= e^{s_i T_s} \\ &= e^{(\alpha_i + j\Omega_i)T_s} \end{aligned} \tag{3}$$

and

$\alpha_i$negative of the damping factor of the i^{th} pole;
$\Omega_i$angular frequency of the i^{th} pole;
$R_i$complex amplitude of the i^{th} pole;
*N*number of data samples;
*M*number of poles of the signal.

The problem reduces to finding the best estimates for M, R_i, and z_i, $i = 1, \cdots, M$. This problem can be solved in various ways. Prony's method [10] and the matrix pencil [11] are amongst the most popular. The matrix pencil method is computationally more efficient and more robust to noise. Details of the proof are available in [12]. In this paper we shall consider the matrix pencil method.

Define two matrices Y_1 and Y_2

$$[Y_1] = \begin{bmatrix} y_1 & y_2 & \cdots & y_L \\ y_2 & y_3 & \cdots & y_{L+1} \\ \vdots & \vdots & \ddots & \vdots \\ y_{N-L} & y_{N-L+1} & \cdots & y_{N-1} \end{bmatrix}_{(N-L)\times L} \tag{4}$$

$$[Y_2] = \begin{bmatrix} y_0 & y_1 & \cdots & y_{L-1} \\ y_1 & y_2 & \cdots & y_L \\ \vdots & \vdots & \ddots & \vdots \\ y_{N-L-1} & y_{N-L} & \cdots & y_{N-2} \end{bmatrix}_{(N-L)\times L}. \tag{5}$$

These matrices can be written as

$$[Y_1] = [Z_1][R][Z_0][Z_2] \tag{6}$$

$$[Y_2] = [Z_1][R][Z_2] \tag{7}$$

where

$$[Z_1] = \begin{bmatrix} 1 & 1 & \cdots & 1 \\ z_1 & z_2 & \cdots & z_M \\ \vdots & \vdots & \ddots & \vdots \\ z_1^{(N-L-1)} & z_2^{(N-L-1)} & \cdots & z_M^{(N-L-1)} \end{bmatrix}_{(N-L)\times M} \tag{8}$$

$$[Z_2] = \begin{bmatrix} 1 & z_1 & \cdots & z_1^{L-1} \\ 1 & z_2 & \cdots & z_2^{L-1} \\ \vdots & \vdots & \ddots & \vdots \\ 1 & z_M & \cdots & z_M^{L-1} \end{bmatrix}_{M\times L} \tag{9}$$

$$[Z_0] = \begin{bmatrix} z_1 & 0 & \cdots & 0 \\ 0 & z_2 & \cdots & 0 \\ \vdots & \vdots & \ddots & \vdots \\ 0 & 0 & \cdots & z_M \end{bmatrix}_{M\times M} \tag{10}$$

$$[R] = \begin{bmatrix} R_1 & 0 & \cdots & 0 \\ 0 & R_2 & \cdots & 0 \\ \vdots & \vdots & \ddots & \vdots \\ 0 & 0 & \cdots & R_M \end{bmatrix}_{M\times M}. \tag{11}$$

Now, consider the matrix pencil

$$[Y_1] - \lambda[Y_2] = [Z_1][R]\{[Z_0] - \lambda[I]\}[Z_2]. \tag{12}$$

Provided $M \le L \le N - M$, the matrix $[Y_1] - \lambda[Y_2]$ has rank M [13]. However, if $\lambda = z_i$, $i = 1, \cdots, M$ the rank is reduced to $M - 1$. This implies that z_i's are the generalized eigenvalues of the matrix pair $\{[Y_1], [Y_2]\}$. Therefore,

$$[Y_1][r_i] = z_i[Y_2][r_i] \tag{13}$$

where r_i is the generalized eigenvector corresponding to z_i.

Or in the equivalent form

$$\left\{[Y_2]^{\dagger}[Y_1] - z_i[I]\right\}[r_i] = [0] \tag{14}$$

where $[Y_2]^{\dagger}$ is the Moore–Penrose pseudo-inverse of $[Y_2]$ [14]. From (14), we can obtain z_i's from the eigenvalues of $[Y_2]^{\dagger}[Y_1]$. Hence, for the matrix pencil method, the poles are obtained directly as a one-step process.

Once M and z_i's are known, the amplitudes of the modes R_i's are easily solved from the following least squares problem

$$\begin{bmatrix} y_0 \\ y_1 \\ \vdots \\ y_{N-1} \end{bmatrix} = \begin{bmatrix} 1 & 1 & \cdots & 1 \\ z_1 & z_2 & \cdots & z_M \\ \vdots & \vdots & \ddots & \vdots \\ z_1^{N-1} & z_2^{N-1} & \cdots & z_M^{N-1} \end{bmatrix} \begin{bmatrix} R_1 \\ R_2 \\ \vdots \\ R_M \end{bmatrix}. \quad (15)$$

A. Total Least-Squares Matrix Pencil

The procedure detailed above is efficient and yields good results in the absence of numerical errors and random noise in the available data. However, in the applications of matrix pencil to real-life problems, the given data is perturbed from its true value due to numerical errors or noise. In this case, the perturbations corrupt the eigenvalues. This results in errors in all aspects of the solution method—the choice of the number of poles (M), the solution for the poles (z_i) and the amplitudes (R_i).

In the case of noisy data, an alternative and more stable method exists—the total least-squares matrix pencil (TLSMP) method. To explain this method, we begin by defining the matrix

$$[Y] = \begin{bmatrix} y_0 & y_1 & \cdots & y_L \\ y_1 & y_2 & \cdots & y_{L+1} \\ \vdots & \vdots & \ddots & \vdots \\ y_{N-L-1} & y_{N-L} & \cdots & y_{N-1} \end{bmatrix}_{(N-L)\times(L+1)}. \quad (16)$$

Define the singular value decomposition (SVD) of Y as

$$[Y] = [U][\Sigma][V]^T \quad (17)$$

U is the $(N-L)\times(N-L)$ unitary matrix whose columns are the eigenvectors of YY^T. V is the $(L+1)\times(L+1)$ unitary matrix whose columns are the eigenvectors of Y^TY and Σ is the $(N-L)\times(L+1)$ diagonal matrix with the singular values of Y (square root of the eigenvalues of Y^TY) in its main diagonal in descending order.

If the given data y_n were noise free, $[Y]$ would have exactly M nonzero singular values. However, due to the noise, the zero singular values are perturbed. This results in several small nonzero singular values. This error due to the noise can be suppressed by eliminating these spurious singular values from $[\Sigma]$ and the corresponding left and right singular vectors. Define $[\Sigma']$ as the $M\times M$ diagonal matrix with the M largest singular values of $[Y]$ on its main diagonal. Further, define $[U']$ and $[V']$ as submatrices of U and V corresponding to these singular values. Since the singular values of $[Y]$ appear in a descending order in $[\Sigma]$, we can write in MATLAB notation

$$[U'] = [U(:, 1:M)] \quad (18)$$
$$[V'] = [V(:, 1:M)] \quad (19)$$
$$[\Sigma'] = [\Sigma(1:M, 1:M)] \quad (20)$$
$$[Y'] = [U'][\Sigma'][V']^T. \quad (21)$$

Comparing the definition of the matrices $[Y]$ (16), $[Y_1]$ (4), and $[Y_2]$ (5) we obtain

$$[Y] = [c_1, Y_1] = [Y_2, c_{L+1}] \quad (22)$$

where c_i represents the ith column of $[Y]$.

Therefore, using $[Y']$ instead of $[Y]$ in (22) results in filtering the noise in both $[Y_1]$ and $[Y_2]$. From (21) and (22) we can write

$$[Y_1] = [U'][\Sigma'][V_2']^T \quad (23)$$
$$[Y_2] = [U'][\Sigma'][V_1']^T \quad (24)$$

where $[V_1']$ and $[V_2']$ are equal to $[V']$ without the last and the first row, respectively. Using (23) and (24), the poles of the signal (eigenvalues of $[Y_2]^\dagger[Y_1]$) are given by the nonzero eigenvalues of

$$\{[V_1']^T\}^\dagger[V_2']^T$$

which are the same as the eigenvalues of

$$[V_2']^T\{[V_1']^T\}^\dagger.$$

The number of modes M is chosen by the number of dominant singular values in the range

$$\sigma_{\max} > \sigma > 10^{-p}\sigma_{\max}$$

where "p" is the number of significant decimal digits in the data.

The ratio $\sigma/\sigma_{\max}$ as a function of the index (singular value number) can be used to determine the proper value of M for the assumed precision. Practically, if we overestimate M we find spurious modes of small magnitude. These do not severely affect the solution. On the other hand, underestimating M would lead to large errors. Hence, it is always preferable to overestimate M.

Using this better choice of M, we can evaluate the poles z_i and the amplitudes R_i using the previously detailed approach.

III. Numerical Examples

To evaluate the application of the matrix pencil algorithm for the elimination of instabilities inherent in a MOT program, our approach is tested on five examples. A program to evaluate the currents on an arbitrary-shaped closed or open body using the electric field integral equation (EFIE) and triangular patching is used [2]. The triangular patching approximates the surface of the scatterer with a set of adjacent triangles. The current perpendicular to each nonboundary edge is an unknown to be solved. In this paper, we do not discuss the details of the MOT algorithm used. The specifics of the algorithm are available in [2]. Vechinski's algorithm uses an averaging technique to reduce the instabilities, but does not eliminate them. The bodies chosen are a plate, a disk, a sphere, a cube, and a cone-hemisphere combination. All bodies are assumed to be perfectly conducting. Although the program can be used with an arbitrary excitation, we used a linearly

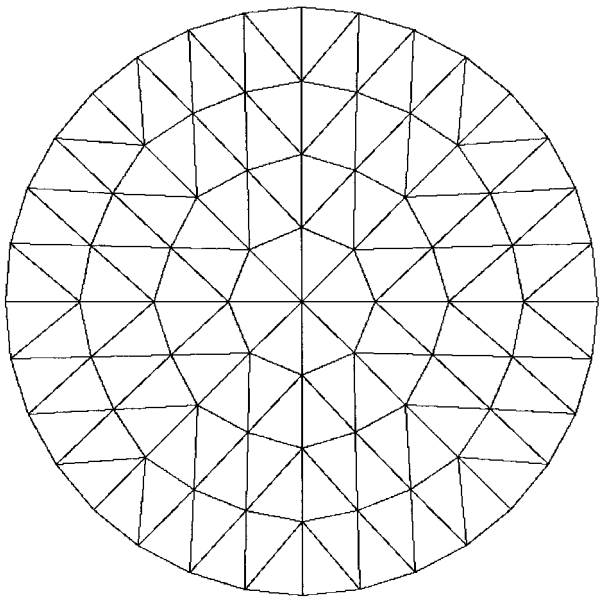

Fig. 1. Triangle patching of a disk.

polarized plane wave with a Gaussian profile in time. The excitation has the form

$$\mathbf{E}^{inc} = \mathbf{u_i} E_0 e^{-(\gamma^2/2)} \tag{25}$$

where

$$\gamma = \frac{t - t_0 - \dfrac{\mathbf{r}.\mathbf{k}}{c}}{\sigma} \tag{26}$$

$\mathbf{u_i}$ is the unit vector that defines the polarization of the incoming plane wave;
E_0 is the amplitude of the incoming wave;
σ controls the width of the pulse;
t_0 is a delay and is used so the pulse rises smoothly from zero for time $t < 0$ to its value at time t;
$\mathbf{r}$ is the position of an arbitrary point in space;
$\mathbf{k}$ is the unit wave vector defining the direction of arrival of the incident pulse.

As mentioned earlier, one of the advantages of using a time-domain formulation is that the bandwidth of the analysis is limited only by the frequency content of the excitation. A discrete Fourier transform (DFT) of the time-domain signal gives the frequency response of the scatterer to the excitation. The DFT is chosen over the quicker fast Fourier transform (FFT) because in a DFT, unlike the FFT, there are no restrictions on the frequency step. To test the validity of this approach, we compare the DFT of the extrapolated time-domain response with the frequency response obtained from a frequency-domain method of moments (MoM) program [15]. The MoM code uses the same triangle patching scheme as the MOT. The MoM code calculates the frequency response of the scatterer. Hence, to compare the two results we multiply the frequency response of the scatterer with the spectrum of the excitation. Fig. 1 shows an example of the triangulation scheme used for a disk.

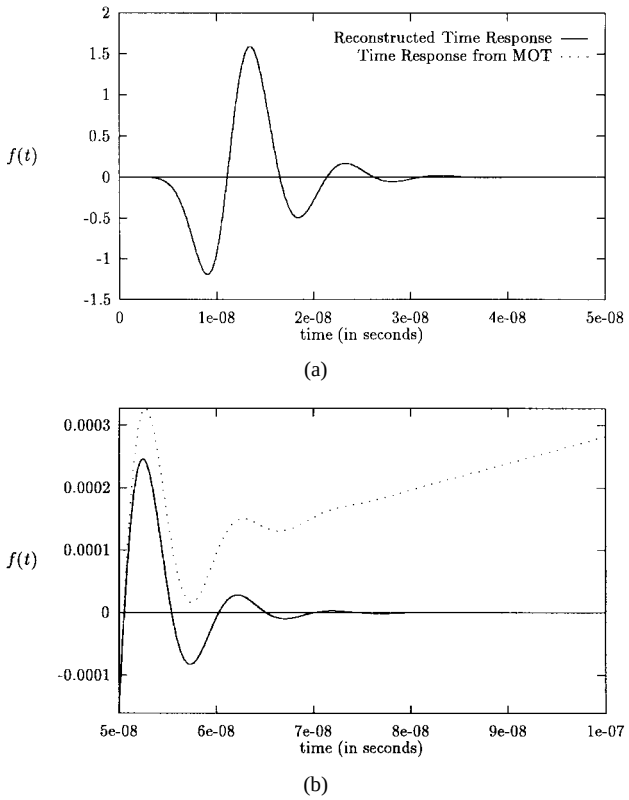

Fig. 2. (a) Early time response. (b) Late time response.

The spectrum of the Gaussian pulse is given by

$$F(j\omega) = \sqrt{2\pi}\sigma e \exp\left\{-\left[\frac{(\omega\sigma)^2}{2} + j\omega t_0\right]\right\}.$$

In all our computations, E_0 is chosen to be 377 V/m. A singular value is considered zero if it less than 10^{-4} times the maximum singular value. This implies that the assumed precision of the given data is four decimal digits using single-precision computation.

In the following sections, the five examples are presented.

Example 1—Square Plate: The first example we present is a square plate of zero thickness and side $1m$ centered at the origin. The plate is located in the xy plane. Eight divisions are made in the x direction and nine in the y direction. By joining the diagonals of each resulting rectangle, 144 triangular patches with 199 unknowns are obtained. This division scheme allows us to evaluate the current at the center of the plate. The excitation arrives from the direction $\theta = 0, \phi = 0$, i.e., along the negative z direction. $\mathbf{u_i}$ is along the x axis. In this example, $\sigma = 2$ns and $t_0 = 10$ns. The time step used in the MOT program is 92.59ps.

In this example, the MOT program evaluates the current for the first 1500 time steps (from $t = 0$ to $t = 0.138\,\mu$ s). Time samples from number 188 ($t = 17.31$ns) to number 233 ($t = 21.48$ns) are used as the input to the matrix pencil program, i.e., $N = 46$. By using $t = 17.31$ ns, the value of the excitation has fallen to less than one-thousandth its maximum value. L in the matrix pencil method is chosen to be 24. After filtering the singular values, the estimate for the number of modes is $M = 2$.

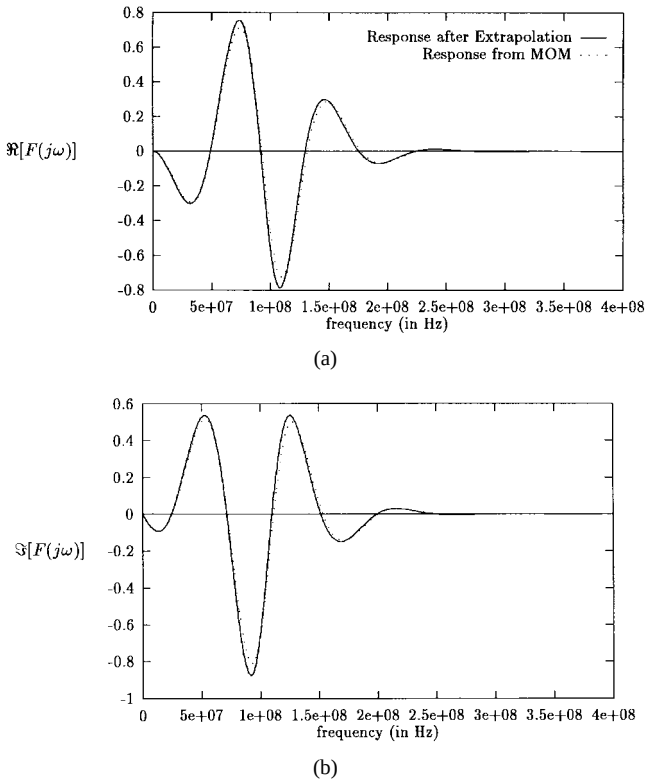

Fig. 3. (a) Real part of the frequency response. (b) Imaginary part of the frequency response.

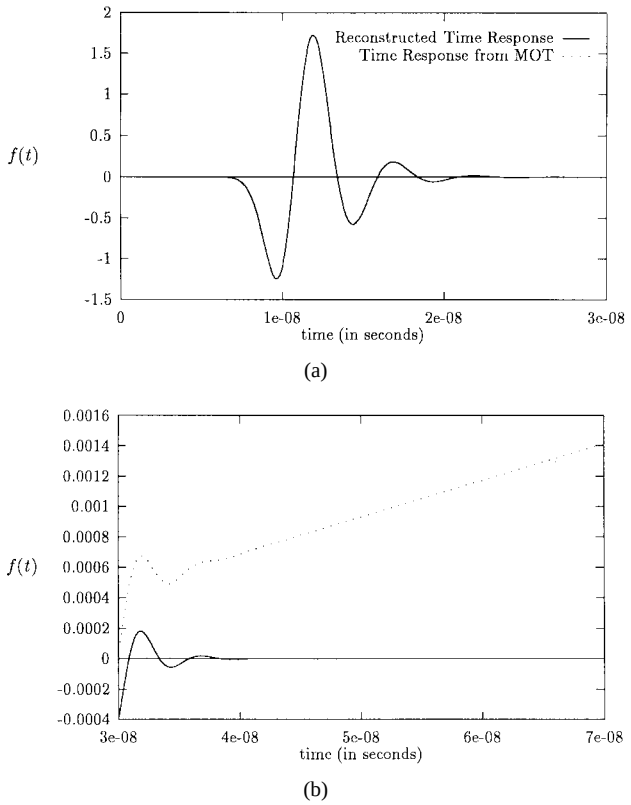

Fig. 4. (a) Early time response. (b) Late time response.

The numerical values of the amplitudes and the exponent of the modes are

$$R_1 = -0.167024 + j0.293158$$
$$z_1 = -2.244\,72 + j6.437\,12$$
$$R_2 = -0.167\,024 - j0.293\,158$$
$$z_2 = -2.244\,72 - j6.437\,12.$$

We see that the amplitudes and the exponents of the two modes are complex conjugates of each other. This guarantees that the resulting extrapolation is real. Also, the real part of the exponents are negative, hence guaranteeing a stable extrapolation.

Using the values for (R_1, z_1) and (R_2, z_2) the current is evaluated from $t = 21.48$ns to $t = 0.138\,\mu$ s. Fig. 2 shows the results for this extrapolation. We compare the results of the matrix pencil extrapolation with the output of the MOT program. Since the data has a large range, the results have been shown from $t = 0$ to $t = 50$ns [Fig. 2(a)] and from $t = 50$ns to 0.138 μ s [Fig. 2(b)]. In Fig. 2(a), we see that where the results of the MOT algorithm are stable, the output of the matrix pencil program is exactly the same. However [as seen from Fig. 2(b)], while the MOT program has started to give erroneous results and the current values appear to be diverging, the matrix pencil produces stable results.

The frequency content of the extrapolated time-domain function are shown in Fig. 3. We evaluate the spectrum of the time-domain response extrapolated by the matrix pencil method, using a DFT, since a FFT would restrict the frequency step that can be chosen. We compare the real and imaginary part of the frequency response with the frequency response obtained from a frequency-domain MoM program. Fig. 3(a) shows the real part while Fig. 3(b) shows the imaginary part of the response. The agreement is within the accuracy of the MoM program.

Example 2—Disk: The next example is a disk of zero thickness, as shown in Fig. 1. The disk lies in the xy plane and is centered at the origin. It has a radius of $0.3m$. The triangulation uses 128 triangles resulting in 208 edges. Thirty-two of the edges are boundary edges yielding 176 unknowns. The excitation arrives from $\theta = 0$, $\phi = 0$, i.e., along the negative z direction. $\mathbf{u_i}$ is along the x axis. Here, $\sigma = 1$ns and $t_0 = 10$ns. The time step used is 47.76ps.

The MOT program evaluates the current at the first 1500 time steps (from $t = 0$ to $t = 71.59$ ns). Sixty-six time samples from number 268 ($t = 12.75$ ns) to number 333 ($t = 15.90$ ns) are used as input to the matrix pencil program. The program uses this data to extrapolate the current from $t = 15.90$ns to $t = 71.59$ns. L is chosen to be 34. The required number of modes is four ($M = 4$). The values of the amplitudes and exponents of the modes are

$$R_1 = -0.448306 - j0.459212$$
$$z_1 = -4.628\,63 + j12.6044$$
$$R_2 = -0.448\,306 + j0.459\,212$$
$$z_2 = -4.628\,63 - j12.6044$$
$$R_3 = -0.013\,55 - j0.007\,086$$
$$z_3 = -20.2747 - j16.7159$$
$$R_4 = -0.013\,55 + j0.007\,086$$
$$z_4 = -20.2747 + j16.7159.$$

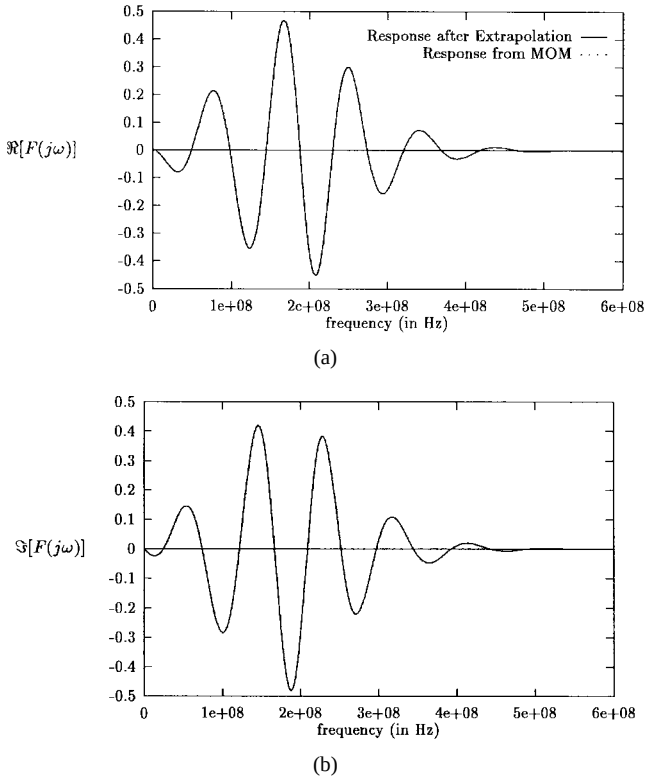

Fig. 5. (a) Real part of the frequency response. (b) Imaginary part of the frequency response.

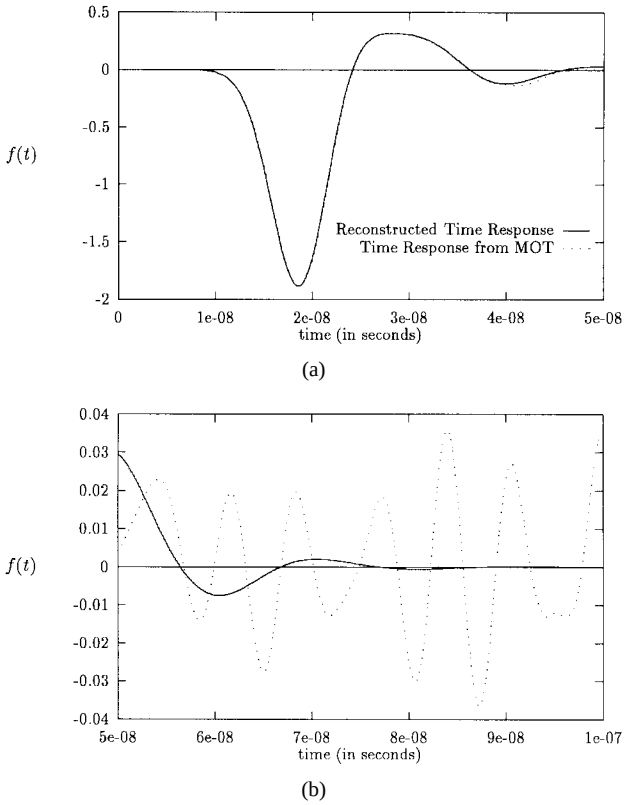

Fig. 6. (a) Early time response. (b) Late time response.

The amplitudes of modes #1 and #2 are conjugates of each other, as are their exponents. This also holds true for modes #3 and #4. Hence, again, the extrapolation is real. Also, all modes have exponents with a negative real part, thus guaranteeing a stable extrapolation. We see that modes #3 and #4 have relatively low amplitude and a very high-damping factor.

We compare the extrapolation with the results of the MOT algorithm. Fig. 4(a) shows the comparison for the early to middle times. The agreement in this region is excellent. Fig. 4(b) shows the comparison of the late time response. We see that while the output of the MOT program has started diverging, the matrix pencil produces stable results.

The frequency response of the disk obtained from the extrapolated time-domain data is shown in Fig. 5. Fig. 5(a) shows the real part, while Fig. 5(b) shows the imaginary part and compared with a MoM code utilizing the frequency-domain EFIE formulation. The two curves are nearly indistinguishable.

Example 3—Sphere: Our next example is a sphere of radius $0.5m$. The sphere is centered at the origin. The "top" half of the sphere ($\theta = 0$ to $\theta = \pi/2$) has six divisions in the θ direction. The first "ring" extends from $\theta = 0$ to $\theta = \pi/16$. The other five rings are equispaced in θ from $\theta = \pi/16$ to $\theta = \pi/2$. Each ring, starting from the top has 6, 16, 20, 24, 28, and 32 triangular patches. The sphere is symmetric with respect to the xy plane. This scheme is chosen so all triangles as close to equilateral as possible. If the ϕ direction were also divided uniformly, the triangles would be skewed. Also, this scheme allows us to evaluate the current at the point (-0.5, 0.0, 0.0).

The excitation arrives from $\theta = \pi/2, \phi = \pi$, i.e., along the x direction. $\mathbf{u_i}$ is along the z axis. In this example $\sigma = 3$ns and $t_0 = 22$ns. The time step used in the MOT program is 0.199 43 ns.

The MOT program evaluated the current for the first 500 time steps (from $t = 0$ to $t = 99.515$ns). Sixty-one time samples from number 123 ($t = 24.131$ns) to number 183 ($t = 36.29$ns) are used as the input to the matrix pencil program. L is chosen to be 32. The estimate for the number of modes (M) is four.

The numerical values of the amplitudes and the exponent of the modes are

$$\begin{aligned} R_1 &= 0.154758 + j0.004330 \\ z_1 &= -1.901\,79 + j5.452\,02 \\ R_2 &= 0.154\,758 - j0.004\,330 \\ z_2 &= -1.901\,79 - j5.452\,02 \\ R_3 &= 0.136\,469 - j0.411\,599\,9 \\ z_3 &= -1.292\,96 + j3.038\,59 \\ R_4 &= 0.136\,469 + j0.411\,599\,9 \\ z_4 &= -1.292\,96 - j3.038\,59. \end{aligned}$$

Using these values of (R_i, z_i), $i = 1 \cdots 4$, the current is evaluated from $t = 36.291$ns to $t = 99.515$ns. We compare the results of the extrapolation with the results of the MOT program in the same time range. Fig. 6 shows the results of this extrapolation. Again, the time axis has been split into two—from $t = 0$ to $t = 50$ns [Fig. 6(a)] and from $t = 50$ns to $t = 100$ns [Fig. 6(b)]. Where the output of the MOT program

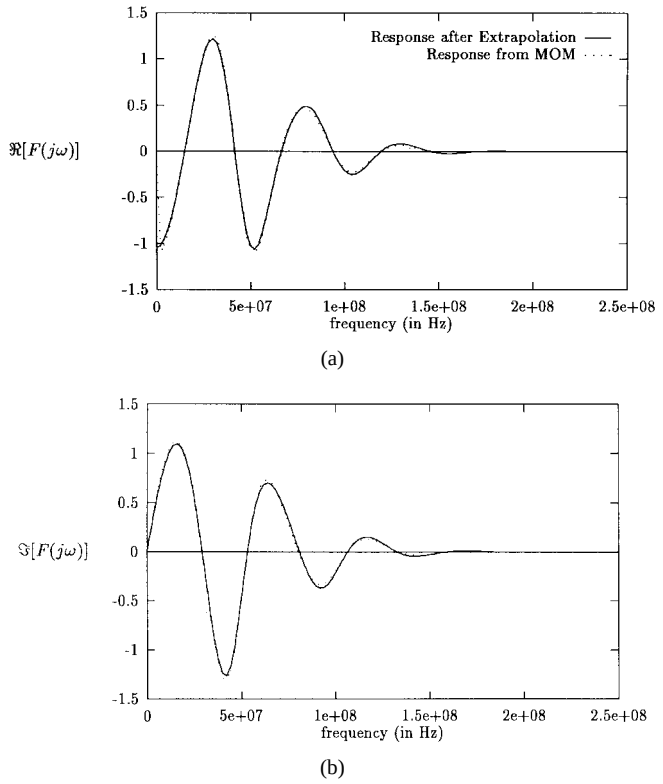

Fig. 7. (a) Real part of the frequency response. (b) Imaginary part of the frequency response.

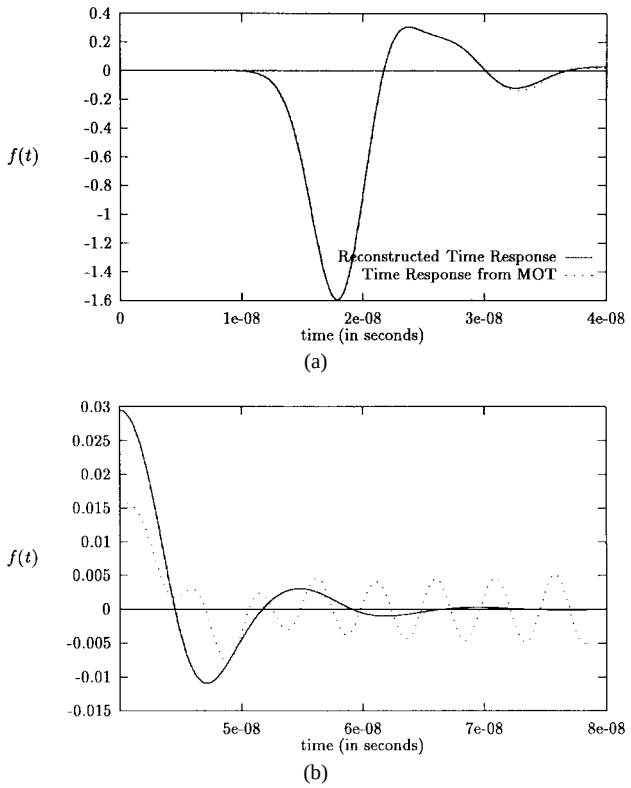

Fig. 8. (a) Early time response. (b) Late time response.

is stable, the two results are indistinguishable. However, for the MOT program, instabilities begin to appear as early as $t = 40$ns. As can be seen from Fig. 6(b), the MOT program gives results that are obviously wrong. The extrapolation using the matrix pencil, on the other hand, continues to be stable.

Next, we compare the frequency content of the extrapolated time-domain results utilizing the matrix pencil approach with the frequency-domain results obtained from the MoM program. Fig. 7(a) shows the real part of the frequency response. Fig. 7(b) shows the imaginary part of the response. In both cases, the agreement is excellent.

Example 4—Cube: The fourth example is a cube of side $1m$ centered at the origin. The faces of the cube are lined along the three coordinate axes. The faces at $x = 0.5$ m and $x = -0.5$ m have five divisions in the y and z direction. All other faces have four divisions in one direction and five in the other. This allows us to find the current at the center of the top face. The excitation arrives from the direction $\theta = 0$, $\phi = 0$, i.e., along the $-z$ axis. $\mathbf{u_i}$ is along the x axis. In this example, $\sigma = 2.357$ns and $t_0 = 20$ns. The time step chosen for the MOT program is 0.157 13ns.

The MOT program evaluated the current for the first 500 time steps (from $t = 0$ to $t = 78.41$ns). Sixty-four time samples from number 130 ($t = 20.11$ns) to number 193 ($t = 30.17$ns) are as input to the matrix pencil program. L is chosen to be 32. The estimate for the number of modes is four.

The numerical values of the amplitudes and exponents of the modes are

$$\begin{aligned} R_1 &= -0.04925 + j0.130665 \\ z_1 &= -2.215\,33 + j8.957\,93 \\ R_2 &= -0.049\,25 - j0.130\,665 \\ z_2 &= -2.215\,33 - j8.957\,93 \\ R_3 &= -0.311\,722 + j0.251\,171 \\ z_3 &= -1.589\,59 + j4.426\,77 \\ R_4 &= -0.311\,722 - j0.251\,171 \\ z_4 &= -1.589\,59 - j4.426\,77. \end{aligned}$$

Using these values for (R_i, z_i), $i = 1, \cdots, 4$, the current at the center of the top face is evaluated from $t = 30.17$ns to $t = 78.41$ns. In Fig. 8, we present the comparison between the extrapolated current and that evaluated using the MOT. Fig. 8(a) shows the comparison up to $t = 40$ns. In this region the instabilities in the MOT results have not set in and the extrapolation faithfully reproduces the waveform. In Fig. 8(b) we see that the MOT results are unstable while the matrix pencil extrapolation continues to be stable.

The frequency content of the current waveform is shown in Fig. 9 and compared with the results of the frequency-domain EFIE code. Fig. 9(a) shows the real part of the spectrum, while Fig. 9(b) shows the imaginary part. In both cases, the agreement is very good.

Example 5—Cone-Hemisphere: The final example we have chosen is a combination of a cone and a hemisphere. The hemisphere is attached to the base of the cone forming one compound 3-D object. The base of the cone and hemisphere

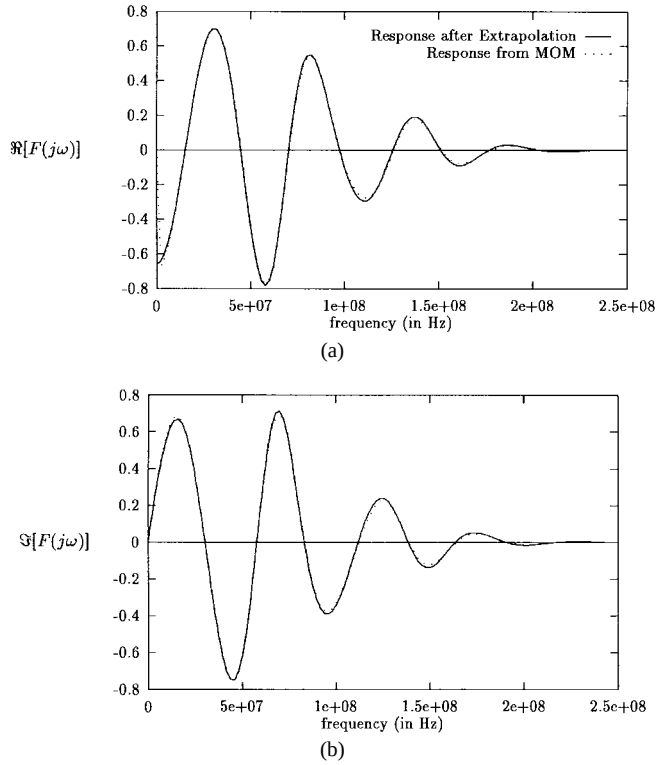

Fig. 9. (a) Real part of the frequency response. (b) Imaginary part of the frequency response.

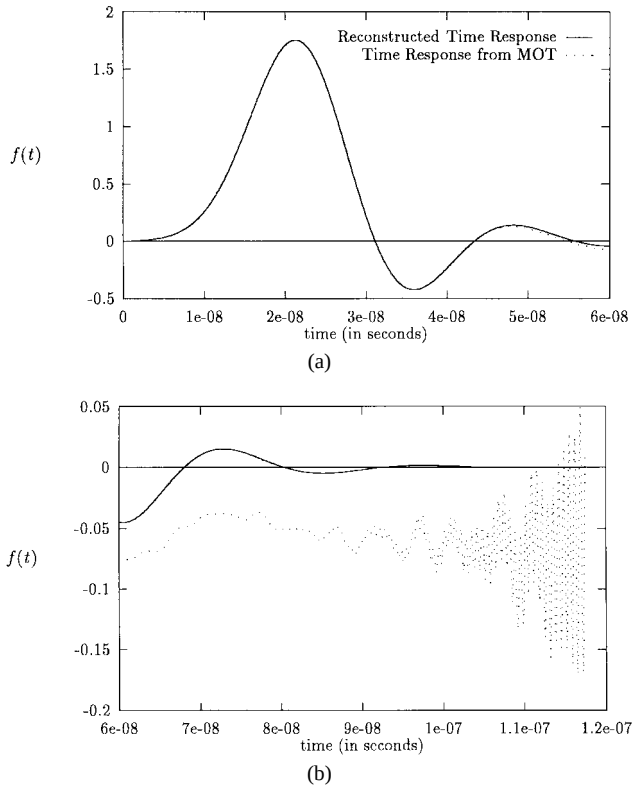

Fig. 10. (a) Early time response. (b) Late time response.

is centered at the origin. The base of the cone and hemisphere have a radius of $1m$. The height of the cone is $2m$. The central axis of the combination lies on the z axis.

The triangular patch approximation for the cone has six divisions in the z direction. The planes defining the "rings"

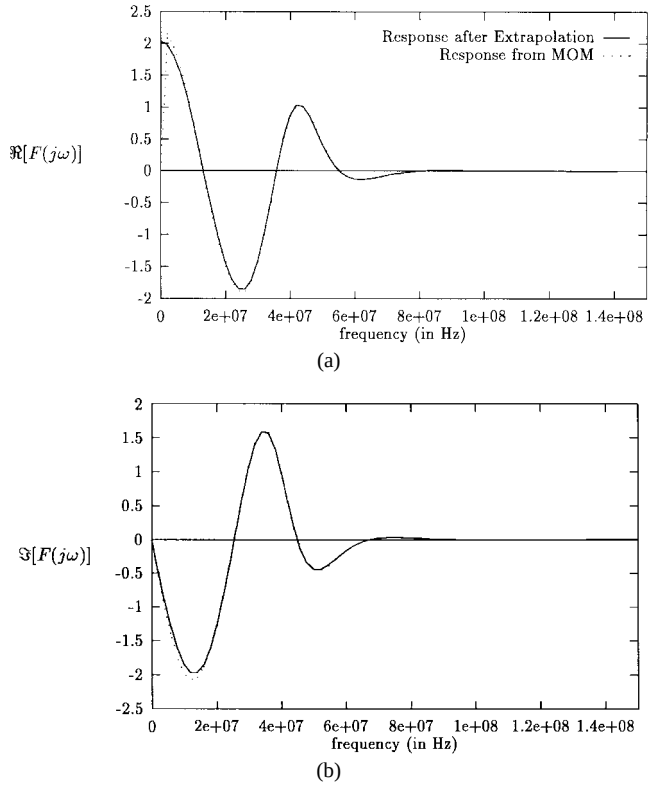

Fig. 11. (a) Real part of the frequency response. (b) Imaginary part of the frequency response.

are at $z = 2.0$, $z = 1.75$, $z = 1.4$, $z = 1.05$, $z = 0.7$, $z = 0.35$, and $z = 0$. Each ring, starting from the top, has 7, 16, 20, 24, 28, and 32 triangles, respectively. The hemisphere has three divisions in the θ direction. The "rings" extend from $\theta = \pi$ to $\theta = 2\pi/3$, $\theta = 5\pi/6$ to $\theta = 2\pi/3$, and $\theta = 2\pi/3$ to $\theta = \pi/2$. Each ring, starting from the bottom, has 13, 28, and 32 triangular patches, respectively. Such a triangulation scheme allows for the current at the point (−0.1, 0.0, 0.0) to be evaluated.

The excitation arrives from $\theta = \pi/2, \phi = \pi$, i.e., along the x direction. $\mathbf{u_i}$ is along the z axis. In this example, $\sigma = 6$ns and $t_0 = 25$ns. The time step used is 90.39ps.

The MOT program evaluated the current for the first 1300 time steps (from $t = 0$ to $t = 0.117\,42\,\mu$ s). One hundred-sixty time samples from number 323 ($t = 29.02$ns) to sample number 482 ($t = 43.48$ns) are used as input to the matrix pencil program. L is chosen to be 60. The estimate for the number of modes (M) is four.

The numerical values of the mode amplitudes and exponents are

$$
\begin{aligned}
R_1 &= -0.205264 + j0.364285 \\
z_1 &= -0.907\,949 + j2.551\,35 \\
R_2 &= -0.205\,264 - j0.364\,285 \\
z_2 &= -0.907\,949 - j2.551\,35 \\
R_3 &= -0.002\,816 + j0.002\,763 \\
z_3 &= -5.644\,74 + j9.755\,56 \\
R_4 &= -0.002\,816 - j0.002\,763 \\
z_4 &= -5.644\,74 - j9.755\,56.
\end{aligned}
$$

Using these values for the amplitudes and exponents, the current values are extrapolated from $t = 43.48$ns to $t = 0.117\,42\,\mu$ s. This is compared with the values obtained from the MOT program. The comparison is shown in Fig. 10. Fig. 10(a) shows the comparison up to $t = 60$ns; in this region, the agreement is very good. Fig. 10(b) shows the comparison from $t = 60$ns to $t = 0.117\,42\,\mu$ s; in this region, the advantage of the matrix pencil program can be clearly seen. The results of the MOT program have already started oscillating and the errors are growing exponentially. However, the results of the matrix pencil are stable.

The frequency response of the time-domain data obtained by the matrix pencil approach of the cone-hemisphere combination can be calculated using the DFT. The comparison between the DFT of the extrapolated time response and the MoM results using a frequency-domain EFIE program is shown in Fig. 11. Fig. 11(a) shows the real part, while Fig. 11(b) shows the imaginary part. In both cases, the agreement is excellent.

IV. Conclusion

In this paper, we have presented the matrix pencil technique to eliminate instabilities arising in a marching-on-time program used to compute the time-domain response of 3-D conducting bodies. We have demonstrated that the instabilities in the computation can be eliminated. The technique presented is robust and can be used even if the given data is noisy.

Since the matrix pencil approach is a signal-processing algorithm, the specific example is irrelevant. The approach works equally well for extrapolating time-domain responses from finite-difference time-domain and time-domain finite-element techniques. The technique presented eliminates the instabilities that are often found in EFIE utilizing a MOT algorithm. The extrapolation of time-domain data using limited time-domain information does provide accurate results as compared to the results obtained independently from frequency-domain MoM codes.

References

[1] E. K. Miller, "Time domain modeling in electromagnetics," *J. Electromagn. Waves Applicat.*, vol. 8, nos. 9–10, pp. 1125–1172, 1994.

[2] D. A. Vechinski, "Direct time-domain analysis of arbitrarily shaped conducting or dielectric structures using patch modeling techniques," Ph.D. thesis, Auburn Univ., 1992.

[3] P. Rynne, "Instabilities in time marching methods for scattering problems," *Electromagn.*, vol. 4, pp. 129–144, 1986.

[4] A. G. Tijhuis, "Toward a stable marching-on-in-time method for two dimensional transient electromagnetic scattering problems," *Radio Sci.*, vol. 19, pp. 1311–1317, 1984.

[5] P. D. Smith, "Instabilities in time-marching methods for scattering: Cause and rectification," *Electromagn.*, vol. 10, pp. 439–451, 1990.

[6] A. G. Tijhuis, *Electromagnetic Inverse Profiling: Theory and Numerical Implementation.* Utrecht, The Netherlands: VNU Sci. Press, 1987.

[7] S. M. Rao, T. K. Sarkar, and S. A. Dianat, "The application of the conjugate gradient method to the solution of transient electromagnetic scattering from thin wires," *Radio Sci.*, vol. 19, no. 5, pp. 1319–1326, Sept./Oct. 1984.

[8] A. Sadigh and E. Arvas, "Treating the instabilities in marching-on-in-time method from a different perspective," *IEEE Trans. Antennas Propagat.*, vol. 41, pp. 1695–1702, Dec. 1993.

[9] C. E. Baum, "The singularity expansion method," in *Transient Electromagnetic Fields*, L. B. Felsen, Ed. New York: Springer-Verlag, 1976.

[10] R. Prony, "Essai experimental et analytique sur les lois de la dilatabilite de fluides elastiques et sur celles del la force expansive de la vapeur de l'alkool a differentes temperatures," *Paris J. I'École Polytech.*, vol. 1, pp. 24–76, 1795.

[11] Y. Hua and T. K. Sarkar, "Matrix pencil method for estimating parameters of exponentially damped/undamped sinusoids in noise," *IEEE Trans. Acoust., Speech, Signal Processing*, vol. 38, pp. 814–824, May 1990.

[12] O. M. Pereira-Filho and T. K. Sarkar, "Using the matrix pencil method to estimate the parameters of a sum of complex exponentials," *IEEE Antennas Propagat. Mag.*, vol. 37, pp. 48–55, 1995.

[13] F. Hu, "The band-pass matrix pencil method for parameter estimation of exponentially damped/undamped sinusoidal signals in noise," Ph.D. thesis, Syracuse Univ., 1990.

[14] G. H. Golub and C. F. Van Loan, *Matrix Computations.* Baltimore, MD: Johns Hopkins Univ. Press, 1989.

[15] S. M. Rao, "Electromagnetic scattering and radiation of arbitrarily shaped surfaces by triangular patch modeling," Ph.D. thesis, Univ. Mississippi, 1978.

Raviraj S. Adve (S'88) was born in Bombay, India. He received the B.Tech. degree in electrical engineering from the Indian Institute of Technology, Bombay, India, in 1990. He is currently working toward the Ph.D. degree at Syracuse University, Syracuse, NY.

His research interests include the applications of adaptive antenna theory to radar systems and wireless communications. He has also investigated the applications of signal processing techniques to numerical and experimental electromagnetics.

Tapan Kumar Sarkar (S'69–M'76–SM'81–F'92) was born in Calcutta, India, on August 2, 1948. He received the B.Tech. degree from the Indian Institute of Technology, Kharagpur, India, in 1969, the M.Sc.E. degree from the University of New Brunswick, Fredericton, Canada, in 1971, and the M.S. and Ph.D. degrees from Syracuse University, Syracuse, NY, both in 1975.

From 1975 to 1976, he was with the TACO Division of the General Instruments Corporation. He was with the Rochester Institute of Technology, Rochester, NY, from 1976 to 1985 and a Research Fellow at the Gordon McKay Laboratory, Harvard University, Cambridge, MA, from 1977 to 1978. He founded OHRN Enterprises, Inc., in 1985, which has been engaged in signal processing research and development with several governmental and industrial organizations. He is also a Professor in the Department of Electrical and Computer Engineering, Syracuse University, Syracuse, NY. He was an Associate Editor for feature articles of the IEEE Antennas and Propagation Society Newsletter and an Associate Editor of the IEEE Transactions on Electromagnetic Compatibility. He is an Associate Editor of the *Journal of Electromagnetic Waves and Applications* and is on the editorial board of the *International Journal of Microwave and Millimeter Wave Computer Aided Engineering*. He has authored or co-authored more than 154 journal articles and conference papers and has written chapters in eight books. His current research interests deal with adaptive polarization processing and numerical solutions of operator equations arising in electromagnetics and signal processing with application to radar system design.

Dr. Sarkar is a Registered Professional Engineer in the New York State and a member of Sigma Xi and International Union of Radio Science Commissions A and B. He obtained one of the "Best Solution" Awards, in May 1977, at the Rome Air Development Center (RADC) Spectral Estimation Workshop. He received the Best Paper Award of the IEEE Transactions on Electromagnetic Compatibility in 1979. He was the Technical Program Chairman for the 1988 IEEE Antennas and Propagation Society International Symposium and URSI Radio Science Meeting. He has been appointed U.S. Research Council Representative to many URSI General Assemblies and is the Chairman of the Intercommission Working Group of International URSI on time-domain metrology.

Odilon Maroja C. Pereira-Filho (S'96) received the B.S.E.E. degree from the Federal University of Pernambuco, Brazil, in 1987 and the M.S.E.E. degree from the Pontifical Catholic University of Rio de Janeiro, Brazil, in 1991. He worked as a research engineer at EMBRATEL—Brazilian Company of Telecommunications from 1988 to 1989 and as a research associate at the Federal University of Pernambuco from March to August 1992. He is currently pursuing the Ph.D. degree at Syracuse University, Syracuse, NY. His main interest is in numerical electromagnetics for CAD applications.

Sadasiva M. Rao, (M'83–SM'90) for photograph and biography, see p. 61 of the January 1991 issue of this TRANSACTIONS.